Scientia Iranica, Vol. 13, No. 2, pp 174–186

SCIENTIA IRANICA

Entrapped Air in Long Water Tunnels During Transition from a Pressurized to Free-Surface Flow Regime

A.R. Kabiri Samani*, S.M. Borghei[1] and M.H. Saidi[2]

Air-water two-phase flow usually occurs during a sudden rise in water level at a tunnel or during the falling of the water level at an upstream reservoir while entering the conduit. When this happens, different flow patterns are generated, due to the hydraulics of flow and fluid properties. An analytical/numerical model, based on the assumption of a rigid incompressible water column and a compressible air bubble, is derived, to simulate pressure fluctuation, void fraction, air/water flow rate and water velocity in a closed conduit, including water depth at the upper reservoir, due to air bubbles becoming trapped in the water, for the highest possible number of flow patterns. It is a comprehensive model, which can generate different hydraulic situations in closed conduits such as tunnels and culverts, based on a hydraulic approach. The boundary conditions are a system of algebraic or/and simple differential equations. The steady solution of the governing differential equations is, generally, performed as the initial data. The frequency of pressure fluctuation and air/water flow rate predicted by the model is in close agreement with the results of the experiments and the numerical model referred to in the literature. Hence, the present model, which is simply derived due to one-dimensional assumptions, shows itself to be a good tool for predicting the characteristics of a two-phase flow.

INTRODUCTION

The study of two-phase fluid flow behavior in hydraulic structures, such as; pressurized flow tunnels, culverts, sewer pipes, bends and other similar conduits, is of great importance. A two-phase mixture flowing in a pipe can exhibit several interfacial geometries, such as: bubbles, slugs and/or films, depending on the fluid and hydrodynamic properties of the flow. The main variables, which can produce a variety of flow patterns, are the relative discharge rate of fluids and the pipe slope. The highest number of flow patterns that are attainable with air and water, are stratified, wavy and slug. The most basic pattern among them is stratified flow. This occurs when water and air flow separately, i.e., water is at the bottom of the pipe and air is over the water with minimum interaction. Then, wavy flow evolves when air flowrate is increased from stratified flow and uniform waves move along the pipe. If air flow is further increased, the wavy water begins to hit the top of the pipe and the result is slug flow.

Ample studies have been conducted to explain and simulate two-phase air-water flow and the effects of air on fluctuation characteristics of flow in a pipeline system. As a result, much effort has been devoted to improving analytical and computational methods for the prediction of local hydraulic conditions in gas/liquid two-phase flows.

The classic work of Martinelli and Nelson [1], assumes the flow regime to be always turbulent and, therefore, have developed a model for pressure drop due to friction. A more useful method in the calculation of flow in a closed conduit is given by Cunge and Wenger [2], based on existing similarities with the Saint-Venant equations between open channel and closed conduit flow. A fictitious narrow slot is added at the top of the pipe so that both free surface and

*. *Corresponding Author, Department of Civil Engineering, Sharif University of Technology, Tehran, I.R. Iran.*

1. *Department of Civil Engineering, Sharif University of Technology, Tehran, I.R. Iran.*
2. *Department of Mechanical Engineering, Sharif University of Technology, Tehran, I.R. Iran.*

pressurized flow can be analyzed by the Saint-Venant equations. The effect of air on fluctuations of flow characteristics in pipeline systems has been of interest to many researchers, such as Holly [3], Albertson and Andrews [4], Martin [5], McCorquodale and Hamam [6] and Li and McCorquodale [7].

Yevejevich [8] pointed out the possibility of trapped air pockets in and the sudden release of an air-water mixture at upstream manholes of storm sewers, during flow transitions. Yen [9] identified the mechanism of transition from free surface to pressurized flow as one type of hydraulic instability in pipelines.

Hamam and McCorquodal [10] proposed a rigid water column approach to model mixed flow pressure transients. The model assumes the water column to be incompressible and the flow uniform but unsteady. An air bubble is trapped inside the water after the occurrence of interfacial instability between air-water flow. Lin and Hanratty [11] studied the criterion for the initiation of slugs with a linear stability theory. The general equations for a two-phase flow have been derived assuming different models, such as homogeneous and separate air-water mixtures. Lockhart and Martinelli [12] have found a correlation between effective parameters for each phase. Their approach is based on the assumption of conventional friction pressure drop equations, which can be applied to each phase of the flow path.

Zhou et al. [13] have investigated flow transients in a rapid filling horizontal pipe containing trapped air in sewer pipes and Woods et al. [14] studied the mechanism of slug formation in downwardly inclined pipes. Soleimani and Hanratty [15] studied the critical liquid flows for the transition from the pseudo-slug and stratified patterns to slug flow. They considered the stability of a stratified flow with a VLW (Viscous Long Wavelength) theory and the stability of a slug, to have an explanation for the observed critical liquid height at the transition to slugging for air and water flowing in a horizontal pipe. Zhang et al. [16] have developed a unified mechanistic model for slug liquid holdup and the transition between slug and dispersed bubble flows.

Issa and Kempf [17] simulated the slug flow in horizontal and nearly horizontal pipes with a two-fluid model. They concluded that when the two-fluid model is invoked, within the confines of the conditions under which it is mathematically well-posed, it is capable of capturing the growth of instabilities in a stratified flow leading to the generation of slugs.

It has been demonstrated by many investigators, both by experimental and numerical methods, that trapped and released air during rapid filling or surcharging can cause a tremendous pressure surge in the system and, eventually, may cause failure in systems. All the above literature indicates that hydraulic instability may occur during the transition from free-surface to pressurized flow in a pipe. Although there are extensive previous works on the instability of water waves inside a closed conduit, there are no exact guidelines or criteria for predicting the effects of the flow. Several studies have been implemented to identify the characteristics of a two-phase liquid-gas flow, especially in fields such as the petroleum industry, but, there is little study on the mechanism and influence of air entrainment into scaled-up water pipelines, such as water tunnels and culverts. Even reviewing reference books and reports, such as USBR manuals [18], for the relation of the headwater (h_1) and discharge of the conduit, shows that there is a gap of knowledge for a certain range of h_1, i.e.; between the upper and lower boundaries of free-surface and pressurized flow conditions. In this range, the sudden change of boundary condition can induce release of an air-water mixture inside the conduit. Since air entrainment causes severe pressure fluctuations, which may damage the pipeline and cause other related problems, such as bursting air bubbles and erosion, detailed study is definitely required. The most interesting property of this kind of flow, which differs from transient flow, such as a water hammer, is that air has a periodic effect on the flow. On the other hand, pressure fluctuations, in a period of time related to the hydraulic properties of the flow, are continuously repeated for constant reservoir headwater.

Issa and Kempf [17] showed that when the compressibility of a gas is included in the calculations, slugs generate more readily and at the right frequency. Thus, more realistic solutions could be reached.

Lack of solid and comprehensive design methods for predicting and calculating the properties of two-phase flow has left engineers without essential information for proper design of two-phase systems, specially in hydraulic structures, such as; pipelines, tunnels and culverts. There is no doubt that much more investigation is needed to increase knowledge of this area of science. Hence, in this study, a new analytical/numerical model has been developed to investigate the effects of both rapid rising and dropping of the water level at a reservoir on the flow through a horizontal or inclined pipe, while the flow is changing from a free surface to pressurized regime and vice-versa. This paper attempts to describe the air bubble and water behavior, applying initial hydraulic properties and one-dimensional flow assumptions. The flow is divided in water columns, which correspond to evolving control volumes. Applying the momentum and continuity equations for each control volume and interface leads to a system of differential equations for each stage of the flow formation. This system of equations can be solved using the Finite Difference (FD) method. In order to assess the results from the analytical model, void fraction, air to water flow rates

(Q_a/Q_w), water velocity and pressure fluctuations are compared with the experimental investigations of Desai and Arsiwalla [19], Zhou et al. [20] and the numerical results of Tarasevich [21].

METHODOLOGY

The transition from pressurized to free-surface flow, which occasionally occurs in water tunnels and culverts, is classified into six stages, as shown in Figure 1. Rigid body theory and deformable control volume were used to obtain the equations of motion for the six stages. For stage 'a', the convectional pressurized flow equation is used. Stage 'd' includes the initiation of instability inside the fluid. It refers to the tendency of the flow to return to its original state after being perturbed, due to the hydraulic properties of flow and fluids. For stage 'f', the flow pattern is stratified, which can be solved using a separate flow model applied to each phase, including the effect of interfacial shear stress.

Apart from stages 'a' and 'f', which are steady and can be solved using the one-phase flow theory, and stage 'd', which is the threshold of instability of water waves, the continuity and momentum equations are developed for stages 'b', 'c' and 'e'. The total differential equations for each stage can be derived and solved, using the FD method. The traveling surge and the stationary air bubble are analyzed continuously during the time, in order to compute pressure fluctuations, velocity and void fraction. In the following, the theory of each stage is developed. The assumptions for the air and water phases are: Application of constant viscosity, no surface tension, a compressible air bubble and an incompressible water column. The reason being that the variety of temperature, which affects the viscosity, is small. The advantage of this approach is that the initiation of air release and the formation of each flow pattern are allowed to occur naturally from any given initial condition. The initial conditions are as part of the calculation for the previous stage and slug flow, automatically, as a product of computation, is developed. Hence, there is no need for phenomenological models.

Pressurized Flow Regime

At this stage, the flow is completely pressurized and usually occurs when $h_1/D \geq 1.5$ (USBR, [18]). Where, h_1 is the upstream reservoir water head and D is the

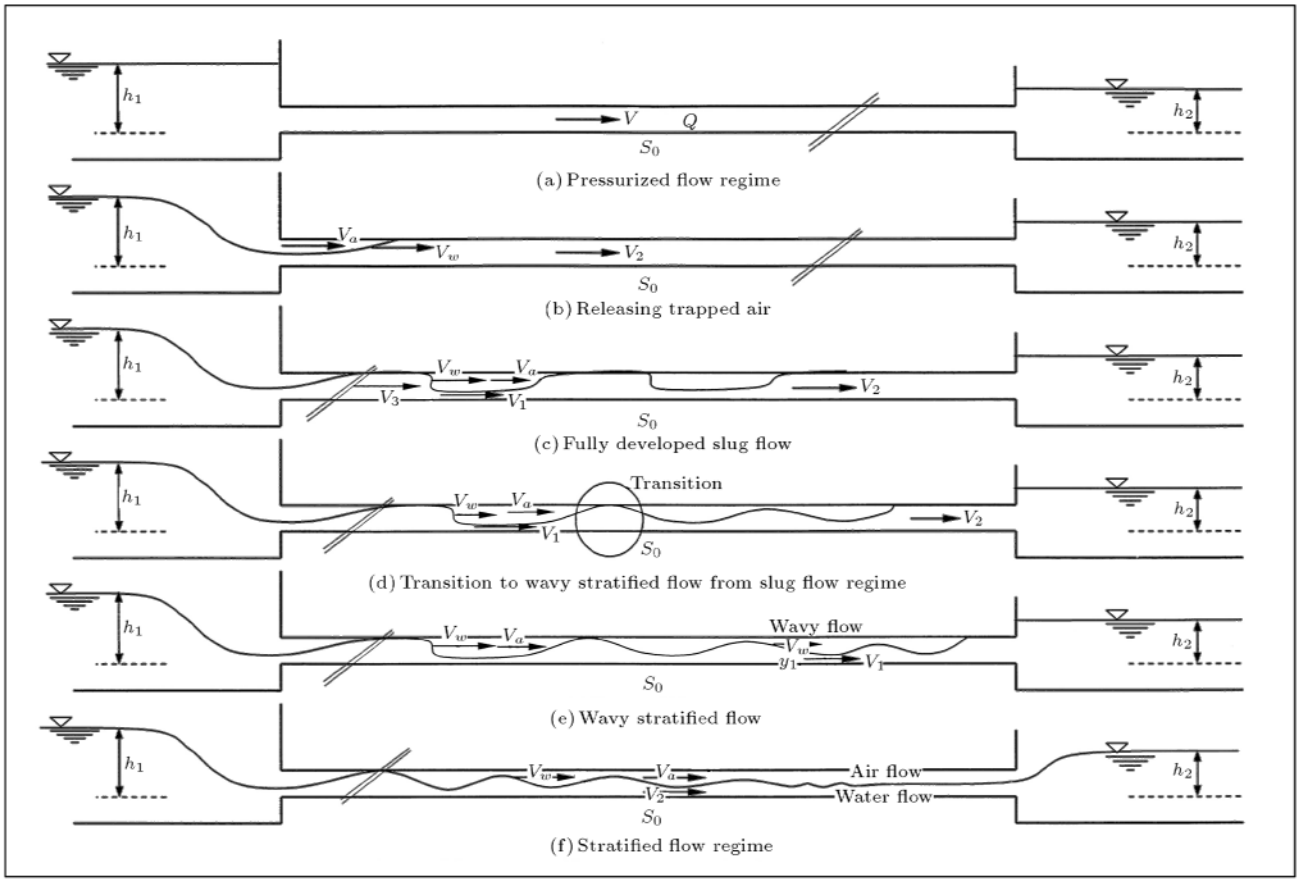

Figure 1. Stages of flow transition from pressurized to free-surface flow.

conduit diameter or height (for a non-circular conduit). The governing equation for the flow is Darcy-Weisbach, Manning or similar relations.

Releasing Air Bubble

The sudden filling of a partially full conduit or the dropping of an upstream reservoir water level, could result in the release of air from the water. When the trapped air bubble reaches the upstream end of the conduit, a sudden release of air may cause severe pressure fluctuations. In order for the trapped air to escape into the atmosphere, the pressure inside the bubble has to exceed a certain threshold. After partial release of air, the pressure inside the bubble drops below the threshold value and the remaining air undergoes compression and expansion. The next release of the air-water mixture occurs when the pressure inside the air bubble drops below the threshold value again. The threshold pressure for air release is related to h_1, (Figure 2) and is equal to:

$$P_t = K_p(h_1 \quad \frac{D}{2})\gamma_w, \tag{1}$$

where P_t is the threshold pressure for air release, K_p is the dimensionless threshold pressure coefficient (equal to 1 [22]) and γ_w is the specific weight of water. The rate of change of air mass of the bubble would be:

$$v_a\frac{d\rho_a}{dt} + \rho_a\frac{dv_a}{dt} = \quad \rho_a Q_a, \tag{2}$$

where v_a, ρ_a and Q_a are volume, density and the discharge of air, respectively. As mentioned, the air bubble is assumed to be compressible, so the relationship between air density and pressure inside the bubble would be:

$$\rho_a = \left(\frac{P_a + P_{\text{atm}}}{C}\right)^{1/\gamma}, \tag{3}$$

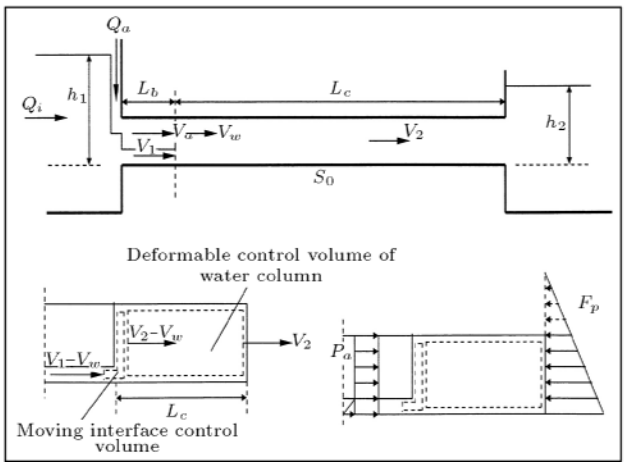

Figure 2. Model and control volume of releasing the first air bubble into water.

where P_a is the air bubble pressure, P_{atm} is the atmospheric pressure and C is constant, which can be determined by substituting the initial amounts of bubble pressure and density (in this study $C = 1.0 \times 10^5$) and $\gamma = 1.2$ [7]. Differentiating Equation 3, with respect to time, gives:

$$\frac{d\rho_a}{dt} = \frac{1}{\gamma C}(\frac{P_a + P_{\text{atm}}}{C})^{1 \quad 1/\gamma}\frac{dP_a}{dt}. \tag{4}$$

Applying the continuity equation to the deformable control volume of water column 1 (Figure 2), gives the rate of change of air bubble volume as:

$$\frac{dv_a}{dt} = V_2 A + A\frac{d(h_1 \quad \frac{D}{2})}{dt} \quad V_w(A \quad A_c), \tag{5}$$

where V_2, A, h_1, V_w and A_c are velocity of water column 1, cross sectional area of conduit, pressure head at upstream, velocity of the moving critical wave and cross sectional area of water column 1, respectively. Also, the rate of air release (Q_a) can be simulated by the orifice equation:

$$Q_a = C_{da}(A \quad A_c)\sqrt{\frac{2P_a}{\rho_a}}, \tag{6}$$

where C_{da} is the air release coefficient and is equal to 0.65 [20]. Combining Equations 2, 4, 5 and 6, the rate of change of pressure inside the bubble becomes:

$$\frac{dP_a}{dt} = \frac{\gamma C}{v_a}(\frac{P_a + P_{\text{atm}}}{C})^{1 \quad 1/\gamma}\Big(\quad \rho_a\Big[V_2 A + A\frac{dh_1}{dt} \quad V_w(A \quad A_c)\Big] \quad \rho_a Q_a\Big). \tag{7}$$

On the other hand, the acceleration of water column 1 (Figure 2) can be derived by applying the continuity and momentum equations to the deformable control volume as:

$$\frac{dV_1}{dt} = \quad gS_0 \quad \frac{f_1 V_1 |V_1|}{8R_1} + \frac{V_1}{A_c L_b}\Big(\quad A\frac{dh_1}{dt} + V_2 A \quad V_w(A \quad A_c)\Big) + \frac{V_2|V_2|}{L_c} \quad \frac{V_2|V_2 \quad V_w|}{L_c} \quad \Big[\frac{P_a(A \quad A_c) + (P_a \quad \frac{P_t}{z})A_c}{\rho_w L_b(A \quad A_c)}\Big], \tag{8}$$

where f_1 is the steady state friction factor (Darcy-Weisbach coefficient) for water column 1, V_1 is the velocity of water column 1, g is the acceleration due to gravity, L_b is the length of air bubble and ρ_w is the density of water. The acceleration of water column 2 can be obtained in a similar form, which will be derived for the next stage. Using the initial conditions, taken at the previous stage, such as discharge and headwater, for the beginning of the air bubble spell, the air release pressure can be calculated by solving Equations 1, 5, 7 and 8, simultaneously.

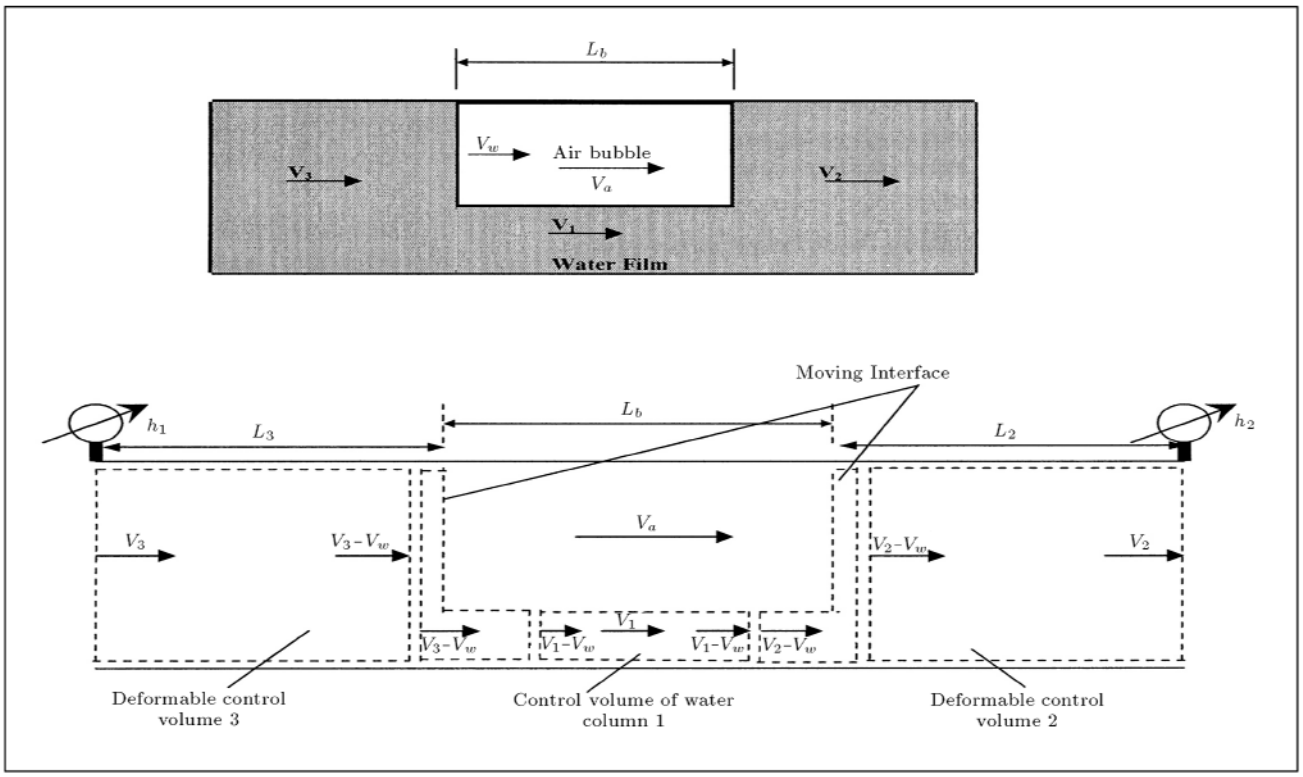

Figure 3. Characteristics of control volume of fully developed slug flow.

Fully Developed Slug Flow

Slug flow is the most complicated pattern in a two-phase flow and includes extreme conditions. McCorquodale and Hamam [6] simulated the transition from free-surface to pressurized flow by assuming a hypothetical, stationary air pocket inside the pipe. Using their assumption on the fully developed slug flow model, the flow is then divided into three rigid water columns with uniform velocities (Figure 3). Each water column is assumed to be enclosed by a fixed control volume. Continuity and momentum equations are then derived for each water column, the interface between columns and the headwater (at the upper reservoir).

It is assumed that the length of water column 1 is constant, so, the fixed control volume approach can be used to derive the continuity and momentum equations. Since water columns 2 and 3 change in size as the air bubble moves downstream, the fixed control volume concept cannot be used. Instead, a deformable control volume should be used to describe them. The general momentum equation for a deformable control volume can be written as:

$$\sum F_e = \frac{\partial}{\partial t}\int_{\text{c.v.}} \rho_w V dv_0 + \int_{\text{c.s.}} \rho_w V V_n dA. \qquad (9)$$

For the acceleration of water column 3, it is assumed that the air pocket travels downstream at a constant velocity, V_b, and the control volume of the column is deforming continuously. The summation of external forces on the rigid water column 3 (Figure 3) is:

$$\sum F_e = \tau_3 \pi D L_3 + A L_3 \gamma_w S_0 + A\gamma_w \Big[h_1 \quad \frac{V_3^2}{2g} \quad K_3 \frac{V_3 |V_3|}{2g}\Big] \quad \rho_w g H A, \qquad (10)$$

where τ_3 is conduit wall shear stress ($\tau_3 = \rho V|V|/2$), L_3 is the length of water column 3, H is the pressure head at the downstream end of water column 3 and K_3 is the loss coefficient of the conduit for water column 3 and is equal to 0.5 for the entrance and 0 otherwise. The right hand side of Equation 9, for water column 3, is:

$$\frac{\partial}{\partial t}\int_{\text{c.v.}} \rho_w V_3 dV_0 + \int_{\text{c.s.}} \rho_w V_3 V_n dA = V_3 \frac{dM_3}{dt} + M_3 \frac{dV_3}{dt} \quad \rho_w V_3 |V_3| A + \rho_w V_3 |V_3 \quad V_w| A. \qquad (11)$$

The rate of change of the mass of Column 3 is $dM_3/dt = \rho_w V_w A$ and the mass of it is $M_3 = \rho_w L_3 A$. Since Equations 10 and 11 are equal, then,

the acceleration of water column 3 would be:

$$\frac{dV_3}{dt} = \frac{g}{L_3}\left[h_1 \quad \frac{V_3^2}{2g} \quad K_3\frac{V_3\,|V_3|}{2g}\right] \quad \frac{P_a + \frac{\gamma_w y_1 A_c}{2A}}{\rho_W L_3} + gS_0$$
$$f_3\frac{V_3\,|V_3|}{8R_3} \quad \frac{V_3\,|V_w|}{L_3} \quad \frac{V_3\,|V_3|}{L_3} + \frac{V_3\,|V_3 \quad V_w|}{L_3}$$
$$\frac{(V_3 \quad V_w)(V_1 \quad V_3)}{L_3}, \tag{12}$$

where f_3 is the steady state friction factor (Darcy-Weisbach coefficient) for water column 3, V_3 is the velocity of water column 3 and y_1 is the depth of water column 1. In the derivation of acceleration of water column 1, the velocity of the moving bubble is superimposed on the fixed length control volume (Figure 3). Applying the momentum equation to the fixed control volume gives:

$$\gamma_w L_b A_1 S_0 \quad \tau_1(\frac{A_1}{R_1})L_b = M_1\frac{dV_1}{dt} + V_1\frac{dM_1}{dt}. \tag{13}$$

As ρ_a is of the 1/1000 order of the ρ_w, so, the air pressure forces, due to friction, can be omitted. Applying equations $(dM_1/dt = \rho_w A(V_3 \quad V_2))$ and $(M_1 = \rho_w A_c L_b)$ for the rate of change of mass and the mass of water column 1, respectively, and substituting these into Equation 13, the acceleration of water column 1 is obtained as follows:

$$\frac{dV_1}{dt} = gS_0 \quad f_1\frac{V_1\,|V_1|}{8R_1} \quad \frac{V_1 A(V_3 \quad V_2)}{A_c L_b}. \tag{14}$$

Acceleration of water column 2 is derived in a similar procedure to that of water column 3. The summation of all external forces at water column 2 (Figure 3) gives:

$$\frac{dV_2}{dt} = \frac{g}{L_2}\left[h_2 \quad \frac{V_2^2}{2g} \quad K_2\frac{V_2\,|V_2|}{2g}\right] + \frac{P_a + \frac{\gamma_w y_1 A_c}{2A}}{\rho_W L_2}$$
$$+ gS_0 \quad f_2\frac{V_2\,|V_2|}{8R_2} + \frac{V_2 V_w}{L_2} + \frac{V_2\,|V_w|}{L_2} \quad \frac{V_2\,|V_2|}{L_2}$$
$$+ \frac{V_2\,|V_2 \quad V_w|}{L_2} \quad \frac{(V_2 \quad V_w)(V_2 \quad V_1)}{L_2}, \tag{15}$$

where f_2 is the friction factor for water column 2 L_2 is the length of water column 2 and K_2 is the loss coefficient of the conduit for water column 2, which is equal to 1.0 for the pipe exit and 0 otherwise. The rate of change of the water level, at the upstream and downstream reservoirs of the conduit, are:

$$\frac{dh_1}{dt} = \frac{Q_i \quad V_3 A}{A_{r1}}, \tag{16}$$

$$\frac{dh_2}{dt} = \frac{V_2 A \quad Q_o}{A_{r2}}, \tag{17}$$

where A_{r1} and A_{r2} are the areas of the upper and lower reservoirs, Q_i is the inflow rate to the upper reservoir and Q_o is the outflow rate from the lower reservoir (If the length of the tunnel is large or water is discharged into the atmosphere, then, dh_2/dt becomes zero).

Applying the continuity equation to the fixed control volume of the air bubble (Figure 3) gives the rate of change of air bubble volume as:

$$\frac{dv_a}{dt} = (V_2 \quad V_3)A \quad Q_a, \tag{18}$$

where Q_a is the air flow rate and is zero, provided no air release mechanism, such as slot, exists along the conduit. Using the ideal gas equation of state with the assumption of a pseudoadiabatic compression and expansion process, the air pressure of the bubble, P_a, is:

$$P_a = P_0(\frac{v_0}{v_a})^\gamma \quad P_{\text{atm}}, \tag{19}$$

where P_0 is the initial absolute air pressure, v_0 is the initial volume of the air bubble and γ is equal to 1.2 for pseudoadiabatic processes. The pressure transients associated with the traveling compressible bubble can be simulated by solving, simultaneously, Equations 12 and 14 to 19, using the FD approach. The initial conditions for the simulation are:

$$P_0 = P_a + P_{\text{atm}}, \tag{20}$$

$$v_a = L_b(A_2 \quad A_c), \tag{21}$$

h_1 and h_2 are taken from the previous stage and V_3 is equal to V_2, also taken from the previous stage.

Transition from Slug to Wavy Stratified Flow

Flow stability is a property of the dynamics of fluid flow. It refers to the tendency of the flow to return to its original state after being perturbed. The dispersion equation, which gives the magnitude of a perturbation as a function of space (x) and time (t), is satisfied by an exponential solution [17],

$$\Psi = \Psi_0 e^{i(kx \quad \omega t)}, \tag{22}$$

ψ stands either for the pressure (p), the density (ρ), the velocity (u) or the void fraction (α). ψ_0 is the amplitude of the original perturbation, k is the complex wave number and ω is the complex frequency.

When the traveling surge pushes air downstream and creates water waves, this may form interface instability, which is usually called Kelvin-Helmholtz instability. When the waves depart from the crown of the conduit, the flow is at the beginning of a change from a pressurized to free-surface regime and, when

the waves hit the top of the conduit, the flow becomes unstable and evolves into slugging. Based on the small amplitude waves between water and air, Milne-Thomson [23] proposed an equation for the instability condition as:

$$|V_a \quad V_w| \geq \sqrt{\frac{\rho_w}{\rho_a}\tanh\left(\frac{2\pi H_a}{L}\right)+\tanh\left(\frac{2\pi H_w}{L}\right)}$$
$$\sqrt{\left(1 \quad \frac{\rho_a}{\rho_w}\right)}\sqrt{\frac{gL}{2\pi}}, \tag{23}$$

where H_a and H_w are hydraulic depth of air and water flow, respectively. Barnea and Taitel [24] used a linear analysis to study the onset of instability for both inviscid and viscous flow, using the "two-fluid model". The criterion they found is:

$$|V_a \quad V_w| < K\sqrt{\frac{\rho_w \quad \rho_a}{\rho_a\rho_w}(\rho_a\alpha_w+\rho_w\alpha_a)g\cos\beta\frac{A}{\frac{dA_w}{dh}}}, \tag{24}$$

where α_a and α_w are gas and liquid fractions, respectively, $K = 1$ for inviscid flow and A and A_w are the pipe and water cross sectional area, respectively.

McCorquodal and Hamam [6], developed the following overall instability criterion for the transition from pressurized to free-surface flow:

$$F_i = \frac{|V_a \quad V_w|}{\sqrt{gH_w}} \geq F_c, \tag{25}$$

where F_i is the interfacial Froude number and F_c is the critical Froude number for the transition from pressurized to free-surface flow. The condition, as stated in Equation 25, is checked during the computation of stage 'c', in order to determine the occurance of interfacial instability and the progress to stage 'e'.

Wavy Stratified Flow

Applying the momentum equation to water column 2 (Figure 1e), the rate of change of velocity would be:

$$\frac{dV_2}{dt} = \frac{gZ \quad V_wV_2}{L} \quad \left[\left(K_e+\frac{fL}{4R_2}\right) \quad 1\right]\frac{V_2^2}{2L}$$
$$\frac{gh_2}{L}+gS_0, \tag{26}$$

where $K_e = 1.0$ is the exit loss coefficient, f is the steady state friction factor and Z is the pressure head on the interfacial instability generation. The velocities superimposed on the control volume of the flow transition yields to:

$$V_w(A \quad A_c) = A_cV_2 \quad AV_2. \tag{27}$$

The conservation of linear momentum on the control volume gives:

$$Z = \quad \frac{A_cy_1}{A}+D+\frac{A_c(V_1 \quad V_2)^2}{g(A \quad A_c)} \quad \frac{P}{\gamma_w}. \tag{28}$$

The corresponding air velocity, V_a, is:

$$V_a = \frac{Q_a}{A \quad A_c}. \tag{29}$$

Equations 26 to 29 are used to simulate the pressure fluctuations in the above regime and can be solved by the FD approach. As for initial conditions; given h_2, V_1 is determined from the Manning's equation of uniform flow and V_2 is determined from Equations 27 and 28.

Gravity Stratified Flow

This is when the flow is almost uniform and the fluid interface is close to a straight line, thus, uniform flow equations can be applied to determine water and air flow rates and velocities, applying the interfacial shear stress in momentum equations. Of course, the "two-fluid model" [25] can also be used for modeling a stratified smooth flow, based on the separated flow model.

RESULTS

This section presents the results of the calculations for the highest possible number of flow patterns using the analytical/numerical model obtained earlier. The aim of the computations is to verify that the model is capable of predicting the initiation, growth and development of slugs in an automatic manner, starting from a steady-state flow (pressurized or free-surface flow) as an initial condition.

The predictions are compared with the various experimental and numerical data of air-water systems, which have been presented by previous researchers. The results presented herein are comprised of each flow regime characteristic, such as; slug velocity, void fraction, pressure fluctuation, variation of discharge due to headwater and variation of water level as a function of inflow and outflow with time.

The comparison between computed and measured data shows good agreement, considering the complexity of two-phase flow regimes and the simplicity of the one-dimensional model.

Figure 4 shows the typical predicted void fraction of a slug flow at a horizontal conduit with time. For this result, the pipe has a 10 cm inner diameter and is 10 m in length. Water and air discharge rates are 4.0 and 1.0 lit/sec, respectively, for a constant h/D of 1.1. The position is taken at the mid-point of the pipe (5 meters from each side). It was seen that the time period of a

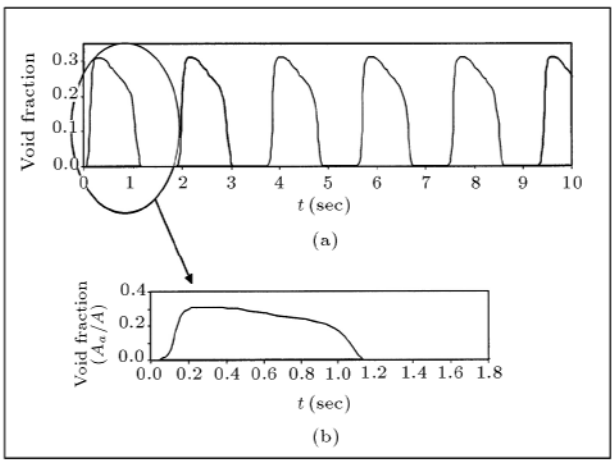

Figure 4. Variation of calculated void fraction as a function of time.

slug surge with this geometry and with these hydraulic conditions is 1.81 sec and the maximum void fraction is 0.3.

Many such computations were carried out with different combinations of water and air flow rates, to establish the conditions under which slug initiates and develops. The flow pattern map predicted by the computations is shown for a horizontal pipe in Figure 5. This figure illustrates the envelopes of water velocity versus air velocity for different possible flow patterns, which occur in a horizontal tunnel. Similar patterns have been introduced using experimental and mathematical results by [25,26]. An interesting result is that by increasing the velocity of air, water velocity decreases in a slug and wavy flow, while, in the case of stratified flow, increasing air velocity has a direct effect on water and increases water velocity too. Although, from Figure 5, general conclusions can be reached, for specific situations, further investigations are needed.

Figure 6 illustrates the measured [19] and calculated void fraction versus air/water discharge ratio.

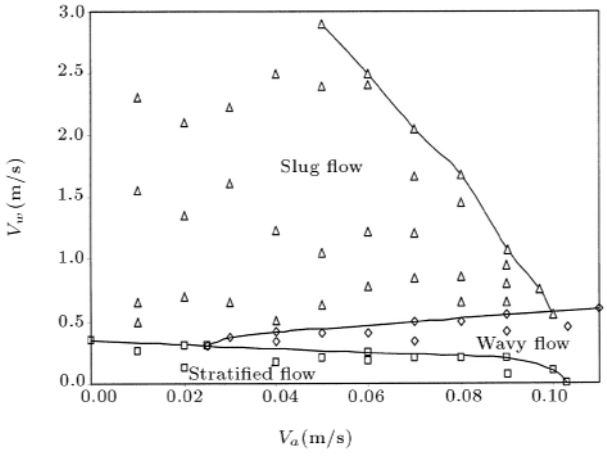

Figure 5. The envelopes of water velocity versus air velocity for different possible flow patterns.

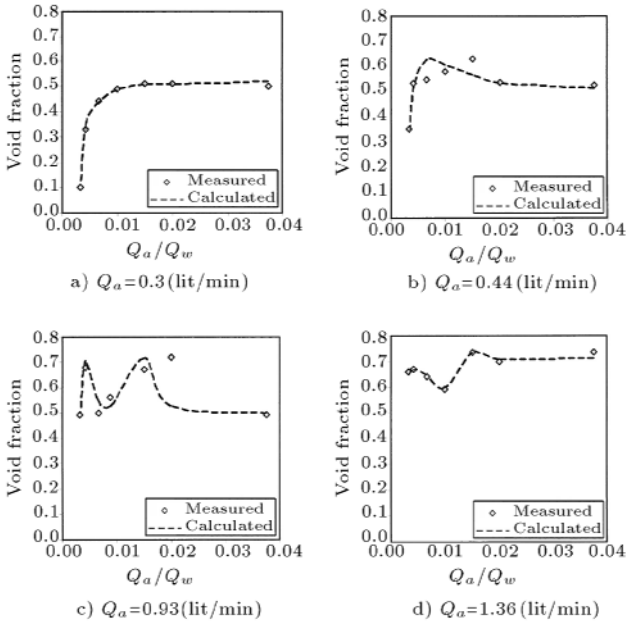

Figure 6. Measured [19] and calculated void fraction versus air/water discharge ratio.

The experimental set-up, which was used to observe the flow patterns of a two-phase flow, consisted of a 270 cm long pipe, with a 2.5 cm inner diameter. The water and air flow rates were obtained by using an orifice plate and a rotameter. To calculate void fraction, the data from [19] were used as primary estimates in the governing equations (Equations 8, 12, 14, 15 and 26) and the air and water velocities and discharges were calculated. The achieved velocities and discharges were used in the conservation of mass equation, then, the void fraction was calculated and compared with the measured data (Figure 7). The four air flow rates, which were used in Figure 6, are 0.3, 0.44, 0.93 and 1.36 lit/min. Figures 7a and 7b compare computed and experimental water velocities and the air/water flow rate ratio, and the experimental data, are given by [19]. Figure 7c compares the measured [19] and calculated void fraction for different air/water flow rates. The majority of the computed results are within a $\pm 10\%$ bound, which is acceptable for experimental data. Thus, the good agreement of the measured and calculated results in these figures shows the applicability of the analytical and numerical solution.

Also, the model is run for the variation of normalized headwater (h_1/D) versus time, for different values of reservoir inflow (the reservoir is assumed to have a fixed area, as shown in Figure 8). The boundaries of this figure are $Q_i = 0$, when there is no inflow to the reservoir and the water level naturally drops, due to pipe discharge (passing the transitional region from pressurized to free-surface flow) and the minimum inflow discharge of $Q_i = 8.5$ lit/sec, which

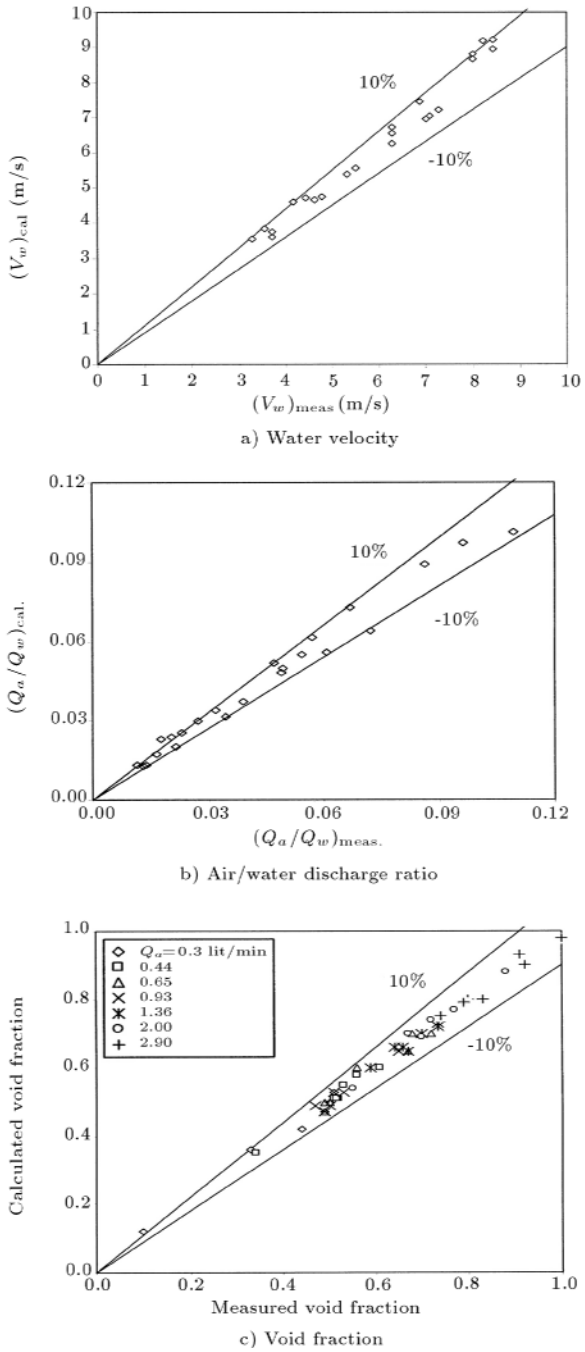

Figure 7. Calculated (present study) versus measured [19] for different parameters.

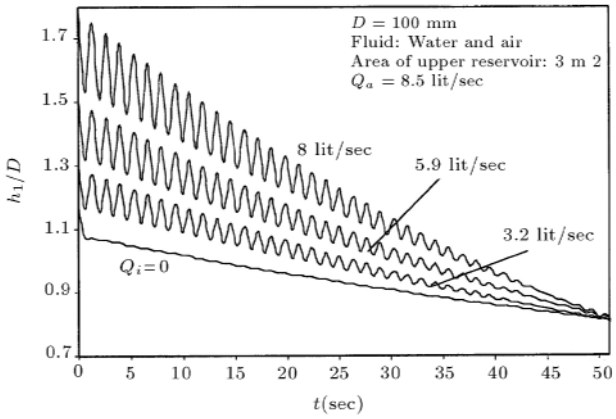

Figure 8. Calculated headwater as a function of time and the inflow discharge to the reservoir.

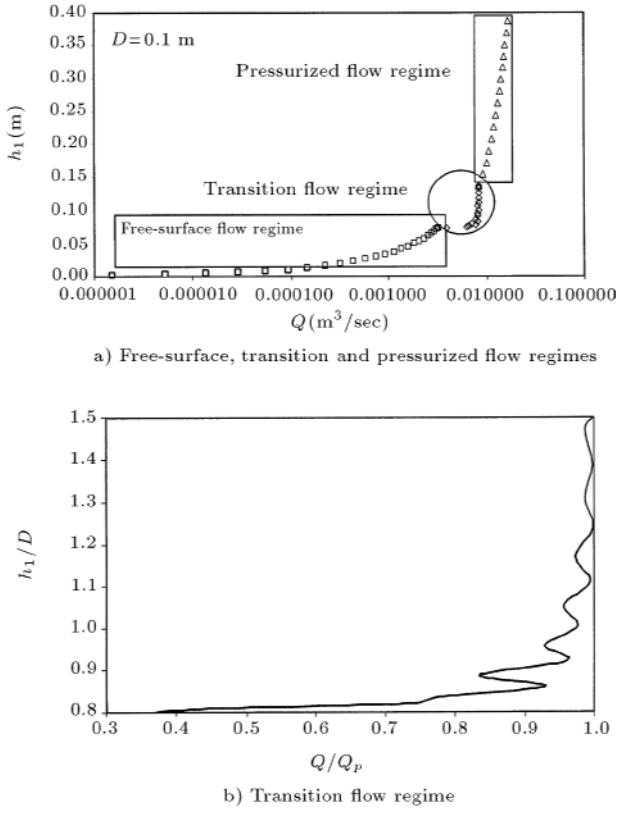

Figure 9. Calculated headwater as a function of pipe flow rate (Equations 12 and 16).

undergoes flow to be pressurized. The pipe's inner diameter is taken as 0.1 m and its length as 10 m. The same geometry is used for Figures 9 and 10. The upper limit of headwater for free-surface flow was 0.8 D and the lower amount for pressurized flow was 1.5 D. Applying these geometrical conditions, the inflow that is the limit for making pressurized flow inside the pipe, is 8.5 lit/sec. Figure 9 illustrates computed headwater as a function of the pipe inflow rate. In this figure, the pressurized and free-surface flow regimes are taken from available equations (Darcy-Weisbach and Manning) and the transition region is calculated by the present model.

Figure 10 shows the calculated headwater as a function of the Froude number (Fr $= Q_w/(gD^5)^{0.5}$) inside the pipe. From Figures 8 to 10, it can be seen that the transition of flow, from pressurized to free-surface, makes the flow wholly unstable. From these figures, it is obtained that increasing the inflow rate, increases the perturbations of headwater and

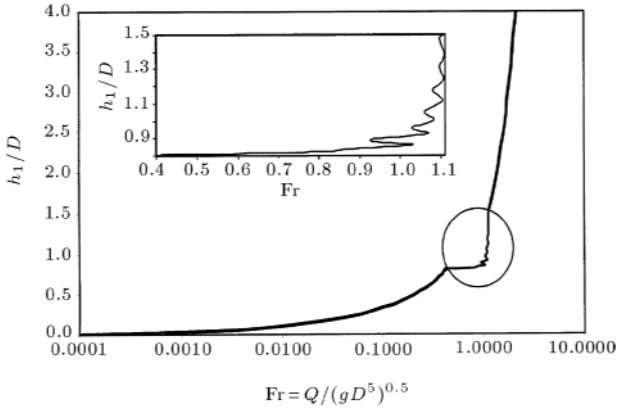

Figure 10. Calculated nondimensional headwater (Equations 12 and 16) as a function of Froude number.

these perturbations will damp more quickly for lower amounts of inflow rate. From another point of view, within these limits, at lower head, the flow tends more towards an increase in discharge against less variation of head while, for higher head, the variation of discharge is less and the head increases rapidly. Therefore, the transition zone is unstable and the flow has a tendency to pass it quickly. The other result to be concluded is that, during transition at the lower water levels, variation in water flow rate is faster, but, at upper water levels, this result is reversed. Beyond a value of 0.82 for headwater, the Froude number is unity and the perturbation initiates. This phenomena is mentioned in [27].

More experimental data and numerical results have been checked with the present model. Figure 11 illustrates calculated and measured [20] pressure fluctuations for stage 'b', in which the first air pocket is released into the water. Zhou et al. [20] studied the effect of an upstream pressure head by implementing two reservoir pressures of 275 and 137 kPa and testing two different initial water column lengths of 5 and

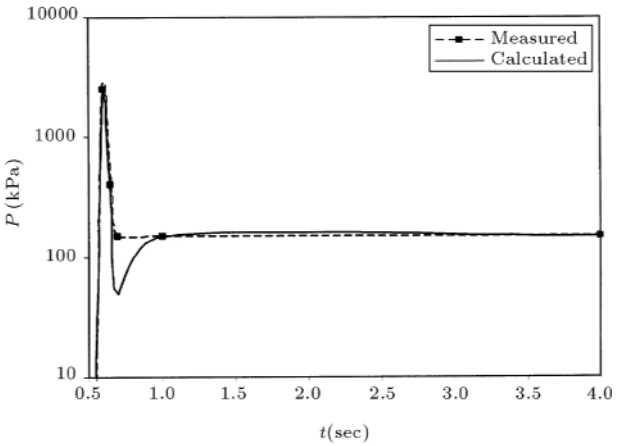

Figure 11. Measured [20] and calculated (Equations 1, 5, 7 and 8) pressure transients by time for releasing trapped air.

8 m. To determine the effects of air release on pressure transients, they tested five orifice diameters of 0, 2, 4, 6 and 9 mm. Their set-up included a simple domestic water supply pressure tank, the pipe being 8.96 m long with an inner diameter of 35 mm and the point of study being the upstream end of the conduit. It can be seen that the pressure suddenly increases up to 10 times that of the hydrostatic pressure. From this figure, a good agreement between results can be seen, except between 0.6 to 0.9 seconds. In this range, the solution diverges locally but, very soon, becomes the same or agrees with measured data. The difference between the results is mainly due to "dissipation error". This type of error usually occurs when the 1st order differential equation is assumed as the governing equation. Even so, the computed and measured data have good agreement within ±10%.

Figure 12a shows the time history of calculated pressure fluctuations using the model developed by the authors and the data calculated with the numerical model of [21]. Tarasevich presented a method of calculation for two-phase flows, based on the method of characteristics. This method uses a two-scale joint grid: One for a liquid phase and the other for a gas phase. It can be seen that the predicted maximum

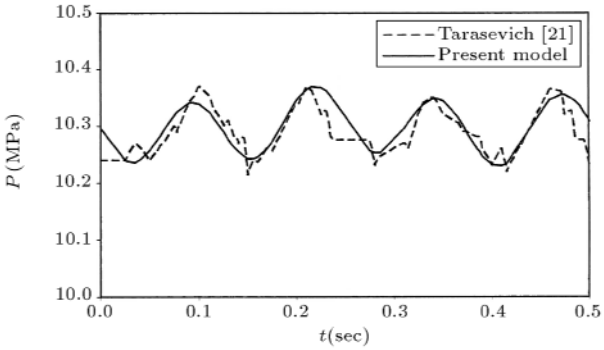

(a) Time dependency of measured [21] and calculated (Equs. 12, 14 to 19) pressure transients for fully developed slug flow regime

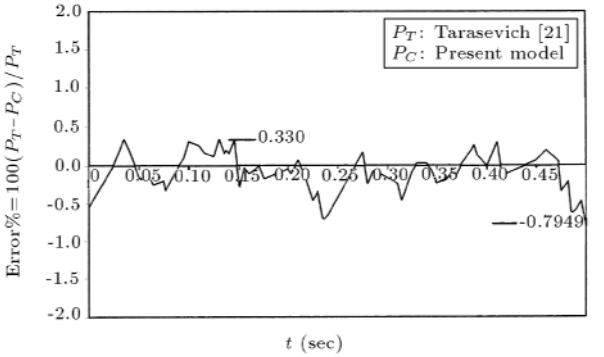

(b) Normalized difference between the measured and calculated

Figure 12. Pressure variation versus time.

Table 1. Design example.

Area (A_{r1}) (m^2)	Inflow (Q_i) (m^3/s)	D (m)	S_0	Q_p (m^3/s)
400000	0	4	0	120

pressure, by the present model, is fairly close to Tarasevich. Although the scatter in results is wider for fully developed slug flow pressure fluctuations, the agreement between the results is fairly good, as seen in Figure 12b. In this figure, the error function, defined as $100(P_T \quad P_C)/P_T$, is shown with time, which is within -0.79 and 0.33 (P_T and P_C are the pressure fluctuations by Tarasevich and the present model, respectively). Since the present model is relatively simple and one-dimensional, it is, therefore, a good tool for predicting an air-water two-phase flow.

CONCLUDING REMARKS

Predicting different two-phase flow patterns is highly necessary to avoid unfavorable situations, likewise, concerning slug flow in systems, which may cause severe wear. The analytical/numerical model, which has been derived to simulate pressure fluctuations, void fraction, air and water velocities and air/water flow rate, due to released air bubbles from the water, is based on the assumption of rigid, incompressible water columns and compressible air bubbles. Since the compressibility of air is important to the generated slugs at the right frequency, the model uses the compressibility of air bubbles. This is a comprehensive model, which can generate different hydraulic situations in a closed conduit, such as tunnels and culverts, based on a hydraulic approach. The boundary conditions are a system of algebraic or/and simple differential equations and the steady solution of the considered problem acts as the initial data.

The results, such as pressure fluctuation and air/water flow rate predicted by the present model, are in close agreement with those recorded in the laboratory experiments (Figures 6, 7 and 11) and numerical results (Figure 12). Hence, the developed model shows to be a good tool with which to predict the characteristics of two-phase flows. Transition of flow from pressurized to free-surface makes flow completely unstable. The other result to be concluded is that, during transition at the lower water levels, the variations of water flow rate is faster, but, at upper water levels, this result is vice-versa. Beyond a value of 0.82 for h_1/D, the Froude number is unity and the perturbation initiates. As the main result of this study, the following relation, to predict the transition time period and headwater fluctuations as functions of inflow to the upper reservoir and pipe discharge, is proposed:

$$\frac{h_1}{D} = \left[0.5366(\frac{Q_i}{Q_p})^2 + 0.03(\frac{Q_i}{Q_p}) + 1.0935\right]$$

$$e^{0.001\left[\ \ 0.5(\frac{Q_i}{Q_p})^2+0.044(\frac{Q_i}{Q_p})\ \ 0.0787\right]t}.e^{\ 0.2i\omega t}$$

$$\frac{dh_1}{dt} = \frac{Q_i \quad Q}{A_{r1}}. \tag{30}$$

Equation 30 is valid for $0.8 \leq h_1/D \leq 1.5$ and $A_{r1} =$ constant (constant area for the reservoir with depth). For example, assume a reservoir and conduit pipe with geometry and hydraulic parameters, as shown in Table 1, with very steep slopes for reservoir walls in order to have a constant area. By substituting these parameters in Equation 30, the transition time from pressurized to free-surface flow is about 8938 sec. This transition will cause severe problems, such as increasing the maximum pressure of the conduit up to 10 times that of the steady-state flow condition and should be avoided or suitably controlled.

ACKNOWLEDGMENT

The authors are grateful for the support of Sharif University of Technology.

NOMENCLATURE

A	cross sectional area of the bottom outlet entrance
A_n	cross sectional area of water columns
A_c	cross sectional area of water column 1 for the releasing air stage
C	constant
C_{da}	the air release coefficient
D	conduit diameter
F_c	critical Froude number for transition of pressurized flow to free surface flow
F_e	external forces acting on the control volume
F_i	interfacial Froude number
H	pressure head at the downstream end of the water column 3
H'	pressure head at the upstream end of the water column 2
H_a	hydraulic depth of air flow

H_w	hydraulic depth of water flow
K_n	loss coefficient of the conduit for columns
K_e	exit loss coefficient
K_p	threshold pressure coefficient (dimensionless)
L	length of interfacial instability wave
L_n	length of water columns
L_b	length of air bubble or water column 1
M_n	mass of water columns
P	air pressure in front of the interfacial instability wave
P_0	initial absolute air pressure
P_C	pressure fluctuations calculated by the present model
P_T	pressure fluctuations calculated by Tarasevich
P_a	air pressure inside the air bubble
P_{atm}	atmospheric pressure
P_t	threshold pressure for air release
Q_1	inflow at upstream end of bottom outlet
Q_a	rate of air release
R_n	hydraulic radius of water columns
S_0	conduit slope
V	flow velocity
V_n	velocity of water columns
V_w	velocity of the moving critical wave (interfacial instability wave)
Z	pressure head on the interfacial instability generation
f	friction factor of the conduit wall
f_n	steady-state friction factor of water columns
h_1	pressure head at bubble front of a slug flow
h_2	pressure head at slug front of a slug flow
v_0	initial volume of the air bubble
v_a	volume of the air bubble
y_n	depth of water columns
γ	a constant equal to 1.2 for pseudoadiabatic processes
γ_w	specific weight of water
ρ_a	air density inside the bubble
τ_n	wall shear stress of water columns
c.s.	control surface
c.v.	control volume
n	the subscript which notates different water columns and is equal to 1, 2, and 3

REFERENCES

1. Martinelli, R.C. and Nelson, D.B. "Prediction of pressure drop during forced circulation boiling of water", *Trans. ASME*, **70**(695) (1948).
2. Cunge, J.A. and Wenger, M. "Numerical integration of Saint-Venant's flow equations by means of an implicit scheme of finite differences", *Application to the Case of Alternately Free and Pressurized Flow in a Tunnel*, La Houille Blanche, (1), pp 33-39 (1964).
3. Holly, E.R. "Surging in laboratory pipeline with steady inflow", *ASCE Journal of Hydraulic Eng.*, **95**(3), pp 961-979 (1969).
4. Albertson, M.L. and Andrews, J.S. "Transients caused by air release", in *Control of Flow in Closed Conduits*, J.P. Tullis, Ed., Colorado State University, Fort Collins, Colorado, USA, pp 315-340 (1971).
5. Martin, C.S. "Entrapped air in pipelines", *Proc. of the 2nd Int. Conf. on Pressure Surges*, BHRA Fluid Eng., London, UK (Sept. 22-24, 1976).
6. McCorquodale, J.A. and Hamam, M.A. "Modeling surcharged flow in sewers", *Proc. Int. Symp. on Urban Hydrology, Hydraulics and Sediment Control*, Univ. of Kentucky, Lexington, Kentucky, USA, pp 331-338 (1982).
7. Li, J. and McCorquodale, J.A. "Modeling mixed flow in storm sewers", *Jou. Hyd. Eng.*, **125**(11), pp 1170-1179 (1999).
8. Yevejevich, V. "Storm-drain network", *Unsteady Flow in Open Channel*, Water Research Publications, Littleton, Colorado, USA, pp 669-703 (1975).
9. Yen, B.C. "Hydraulic instabilities of storm sewer flows", *Proc. Conf. on Urban Drainage*, University of Southampton, Southampton, UK, pp 283-293 (1978).
10. Hamam, M.A. and McCorquodale, J.A. "Transient conditions in the transition from gravity to surcharged sewer flow", *Canadian Journal of Civil Engineering*, **9**(2), pp 189-196 (1982).
11. Lin, P.Y. and Hanratty, T.J. "Prediction of the initiation of slugs with linear stability theory", *Int. J. Multiphase Flow*, **12**, pp 79-98 (1986).
12. Lockhart, R.W. and Martinelli, R.C. "Proposed correlation of data for isothermal two-phase two-component flow in pipes", *Chem. Eng. Prog*, **64**(193) (1949).
13. Zhou, F., Hicks, F. and Steffler, P., "Sewer rupture due to pressure oscillations in trapped air pockets", *CSCE General Conference*, Canada, **II**, pp 491-500 (1999).
14. Woods, B.D., Hurlburt, E.T. and Hanratty, T.J. "Mechanism of slug formation in downwardly inclined pipes", *Int. J. Multiphase Flow*, **26**, pp 977-998 (2000).
15. Soleimani, A. and Hanratty, T.J. "Critical liquid flows for the transition from the pseudo-slug and stratified patterns to slug flow", *Int. J. Multiphase Flow*, **29**, pp 51-67 (2003).
16. Zhang, H.Q., Sarica, W.Q.C. and Brill, P.J. "A unified mechanistic model for slug liquid holdup and transition between slug and dispersed bubble flows", *Int. J. Multiphase Flow*, **29**, pp 97-107 (2003).

17. Issa, R.I. and Kempf, M.H.W. "Simulation of slug flow in horizontal and nearly horizontal pipes with the two-fluid model", *Int. J. Multiphase Flow*, **29**, pp 69-95 (2003).

18. "USBR", *Design of Small Canal Structures*, Bureau of Reclamation, United States Department of the Interior, Denver, Colorado, USA (1978).

19. Desai, A. and Arsiwalla, H. "Flow patterns in two phase flow. chE 390", *Progress Report 3. Project 1*, Chemical Eng. Uiuc. Edu. (2000).

20. Zhou, F., Hicks, F. and Steffler, P., "Effects of trapped air during rapid filling of partially full pipes", *Annual Conference of the Canadian Society for Civil Eng.*, Canada (2002).

21. Tarasevich, V.V. "The calculation of the flows of two-phase mixtures in pipe systems", *Proc. 1st All-Russia Seminar about Dynamics of Space and Nonequilibrium Flows of Liquid and Gas*, Russia, pp 111-113 (1993).

22. Savary, C.N.B., Aimable, R. and Zech, Y. "Numerical modeling of air-water flow forced by downstream pressure rise in culverts", *Proc. XXX IAHR Congress, Theme B*, pp 495-502 (2003).

23. Milne-Thomson, L.M., *Theoretical Hydrodynamics*, McMillan, New York, USA (1938).

24. Barnea, D. and Taitel, Y. "Interfacial and structural stability of separated flow", *Int. J. Multiphase Flow*, **20**, pp 387-414 (1994).

25. Levy, S. "Two-phase flow in complex systems", John Wiley & Sons, Inc., New York, USA (1999).

26. Collier, J.G., *Convective Boiling and Condensation*, 3rd Ed., Clarendon Press, Oxford, UK (1996).

27. French, R.H., *Open Channel Hydraulics*, McGraw-Hill Book Company, New York, USA (1985).